

Confinement and Stability of Plasmas in a Field-Reversed Configuration

J. T. Slough, A. L. Hoffman, R. D. Milroy, and E. A. Crawford
STI Optronics, Bellevue, Washington 98004

M. Cecik, R. Maqueda, and G. A. Wurden
University of Washington, Seattle, Washington 98195

Y. Ito and A. Shiokawa
Osaka University, Osaka, Japan
 (Received 21 May 1992)

Experiments have been conducted on the LSX device where plasmas confined in a field-reversed magnetic geometry have exhibited record energy, particle, and configuration lifetimes. The scaling from previous smaller devices showed a very positive confinement scaling with s , the number of ion gyroradii inside the field-reversed configuration. These plasmas were observed to have gross stability to global low-order modes such as the internal tilt. The growth of tilt instabilities was not observed during the equilibrium decay of plasmas up to $s \sim 8$.

PACS numbers: 52.55.Pi

A new experimental device (LSX) has been constructed to explore the confinement and stability of magnetically confined plasma known as a field-reversed configuration (FRC). An FRC has a compact toroidal confinement geometry where induced toroidal diamagnetic currents generate the confining poloidal field [1]. Since the toroidal field is typically small inside the FRC, the configuration has an intrinsically high plasma β (the magnetic field vanishes at the plasma core). This feature together with the simple cylindrical geometry, the natural diverter nature of the external magnetic field, and the ease of translation [2] give the FRC unique advantages as a fusion reactor—particularly for advanced fuels [3].

From a theoretical point of view, the key issue has been the gross stability of the configuration. For several years it has been known that the FRC equilibrium, as a result of the unfavorable curvature of the closed field lines (see Fig. 1), is unstable in the magnetohydrodynamic (MHD) limit. In particular, the FRC is unstable to the internal tilt instability [4]. This global mode consists of a rotation of the FRC orthogonal to the symmetry axis with only a small distortion to the separatrix shape, and thus cannot be suppressed by the application of an external magnetic field. The mode has a growth rate that would annihilate the configuration on the shortest possible MHD time

scale, the time for an Alfvén wave to propagate the half length of the FRC.

Stability for many Alfvén transit times has been observed in several FRC experiments [1,5]. The FRC's formed in these experiments, however, had a strong kinetic particle component. This component can be characterized by the parameter s , the average number of ion gyroradii between the null and separatrix of the FRC, and s was typically 2 or less. It was shown that for $s < 2$, kinetic effects significantly increased the MHD tilt growth time [6] to as long as the FRC configuration lifetimes obtained at that time. Subsequent experiments on the TRX device, however, indicated stability to the tilt at moderate s (2 to 4) for many kinetically increased tilt growth times [5]. The confinement did not improve with increasing s as had been observed in previous low- s , kinetic-regime experiments. It was not determined what limited confinement; however, the equilibria produced in these large- s experiments were different in that the radial density profile appeared much flatter than observed at lower s . Recently, experiments were conducted on the FRX-C/LSM device [7], a device of similar coil radius ($R_c = 0.35$ m) to LSX ($R_c = 0.45$ m), where the FRC confinement actually degraded as s was increased above 2. B_θ probe arrays indicated a significant increase in signal amplitude for s/E above 0.5 (where E is the FRC elongation $E = l_s/2r_s$ which was typically about 4 in these experiments).

Based on the low- s empirical confinement scaling, a reactor would require an s value of at least 20. It was thus generally thought that FRC equilibria with s values above 2 would require some augmentation of the kinetic effects, which could perhaps be supplied by energetic neutral beams. Although no such augmentation was provided in the LSX experiments, both stability and positive confinement scaling were observed well into the MHD regime.

LSX is a field-reversed theta pinch, with several addi-

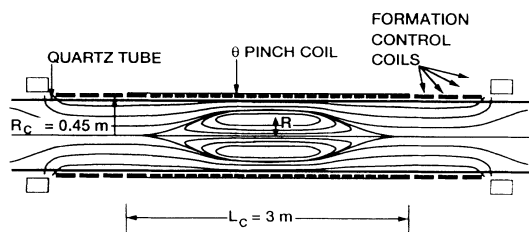


FIG. 1. Schematic of the LSX experiment. Equilibrium flux contours are shown from a 2D numerical calculation for an FRC in LSX.

tional magnetic coils that are used to control the formation of the FRC. The magnetic geometry is illustrated in Fig. 1. The process of FRC formation is begun by completely ionizing a deuterium gas (0.5 to 20 mTorr) in the presence of an axial bias magnetic field, such that the field is imbedded in the plasma in a quiescent and uniform manner. The external magnetic field is then reversed on a time scale shorter than the resistive diffusion time of the bias field from the plasma which allows for the formation of the configuration shown in Fig. 1.

Production of FRCs in a large theta pinch such as LSX is made difficult by the requirement that the plasma be heated from a few eV temperature prior to field reversal, to at least several hundred eV at peak magnetic compression 20 μ sec later. The plasma must also be distributed radially and axially into a quiescent equilibrium on this same time scale as well, which is roughly an axial Alfvén time. It was found essential that this process be carefully controlled in order to achieve an equilibrium FRC in LSX, particularly in the more MHD-like regime with $s > 2$ [8]. The formation techniques required to form FRC equilibria with radially peaked density profiles, which characterized the FRCs with the best confinement, will be detailed elsewhere. Under optimum formation sequencing, FRC equilibria characterized by s values as large as 5 could be generated. Good confinement was observed at all s values; however, the proper equilibria became more difficult to establish at larger s . For a typical rigid-rotor, radial FRC profile, $s \approx 0.3R^2/\rho_i R_c$, where R is the FRC major radius and ρ_i is the ion gyroradius near the FRC separatrix. The particle confinement time τ_N for optimum equilibria is plotted as a function of the s parameter in Fig. 2. The data from other experiments

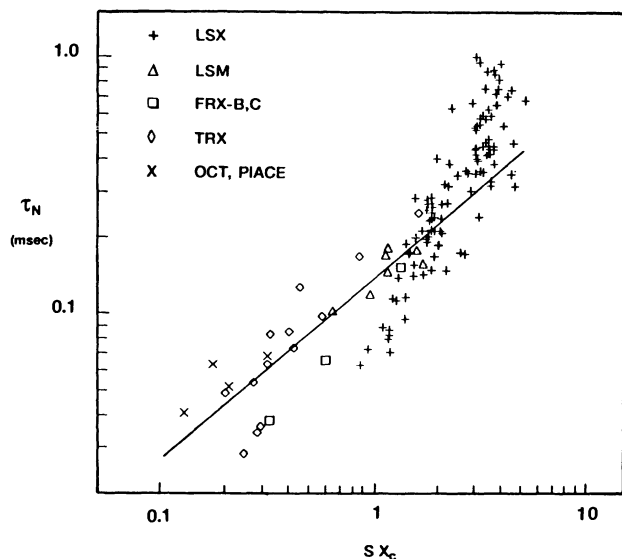


FIG. 2. Particle confinement τ_N observed on LSX and other experiments as a function of $s x_c$, where x_c is the ratio of coil radius to LSX coil radius.

reflect an abscissa value that is the product of the s parameter and x_c , the device R_c normalized to the LSX R_c . This allows the abscissa to be interpreted as R^2/ρ_i , a scaling dependence that had been observed in previous device scaling experiments at Los Alamos National Laboratory [9], and consistent with transport predictions based on microturbulence [10]. The line represents the best fit to all experimental data shown *prior* to LSX, and implies $\tau_N \propto (R^2/\rho_i)^{0.7}$. The LSX data indicate a stronger scaling with R . The empirical scaling inferred by the LSX data has $\tau_N \propto s^{1.4}$. This strong scaling dependence at fixed coil radius is similar to that observed before on TRX [11]. The effective diffusion coefficient for the FRCs on LSX at larger s is less than 5 m^2/sec , which is comparable to that achieved in large tokamak experiments.

Data were obtained from a wide range of FRC equilibrium conditions. The diagnostics used to determine those conditions consisted of compensated diamagnetic loop arrays and magnetic probes which were used to provide information on FRC shape, flux, and energy content [1]. Side-on interferometry and plasma continuum emission arrays were used to obtain FRC particle inventory and density profile. On several discharges the electron temperature T_e was determined by Thomson scattering with the scattering volume 7 cm off the coil axis. Total plasma temperature, $T_t = T_e + T_i$, was inferred from radial pressure balance with the external field. Calibrated silicon photodiodes were used to measure the total radiated power from the FRC. End-on multiframe x-ray and visible cameras, as well as an array of 48 external B_θ pickup loops [12], were used to detect FRC separatrix movement and asymmetries. The equilibrium FRC major radii ranged from 0.1 to 0.17 m with the confining magnetic field spanning 0.4 to 0.8 T. Average FRC densities and temperatures ranged from ($n = 5 \times 10^{21} \text{ m}^{-3}$, $T_i = T_e = 0.1 \text{ keV}$) at 20 mTorr to ($n = 8 \times 10^{20} \text{ m}^{-3}$, $T_i = 1.5 \text{ keV}$, $T_e = 0.6 \text{ keV}$) at 0.6 mTorr filling pressures. The latter condition represents a new operating regime for FRCs. The electron temperature measured was found to be significantly higher than previous experiments even with the same pressure balance temperature. This implies a major change in the cross-field thermal transport from that observed previously [13].

The plasma energy confinement was also observed to scale with s . A maximum confinement time τ_E of 0.3 msec was observed using the optimum formation sequence. The average equilibrium parameters are listed in Table I as condition 1. With the improved energy confinement at larger s , the radiated power has become a significant loss channel (see Table I). The radiated power during equilibrium was consistent with line radiation from the same small fraction (0.04%) of silicon impurity observed in previous FRC experiments performed in quartz vacuum chambers [14]. The Z_{eff} determined from doping experiments on LSX was typically 1.3, with

TABLE I. FRC power flow on LSX (MW). P_l is the total power loss; P_r , radiative loss; P_N , particle loss; P_{in} , input into electrons; P_T , loss due to electron cooling. Condition 1: $n_e = 1.8 \times 10^{21} \text{ m}^{-3}$, $T_e \sim T_i = 150 \text{ eV}$, $s = 4.1$, $\tau_\phi = 0.45 \text{ msec}$, $\tau_N = 0.8 \text{ msec}$. Condition 2: $n_e = 1.3 \times 10^{21} \text{ m}^{-3}$, $T_e = 265$, $T_i = 370 \text{ eV}$, $s = 2.2$, $\tau_\phi = 0.15 \text{ msec}$, $\tau_N = 0.20 \text{ msec}$.

	P_l	P_r	P_N	P_{in}	P_T
Condition 1	93	40	59
Condition 2	170	25	143	25	17

oxygen at about 0.3% being the most abundant impurity.

It can be seen from Table I that the total power loss from the FRC, given by the measured total energy confinement τ_E , is accounted for by radiation P_r and particle loss P_N alone ($P_N = 2.5NkT_i/\tau_N$). Since thermal conduction losses have yet to be accounted for, one is led to infer that particles are lost at lower temperature at the separatrix. Classical cross-field ion thermal conduction would produce essentially a flat radial T_i profile, so that an electron temperature gradient at the FRC edge must account for lower electron thermal losses. Support for this conclusion comes from data taken at operating condition 2 in Table I. The energy confinement time τ_E was 0.10 msec at filling pressures between 2 and 3 mTorr. Thomson scattering data were obtained shot to shot during the first 0.06 msec for this condition. No electron temperature decay, other than that expected from adiabatic cooling, was observed for these data. This is consistent with measurements made on other FRC devices [13].

The power flow into the electrons, P_{in} in Table I, includes heating from magnetic compression, Ohmic heating from flux decay, and equilibration heating from the hotter ions. The power lost from electron diffusion and conduction can be written as $(f)kT_e$ per electron. The factor f is a number greater than $\frac{5}{2}$ that accounts for kinetic and ambipolar effects in the edge plasma as it is lost to the open field lines [15]. The mean value of f inferred from previous experiments with similar collisionality is 4.4. A convective model [15] predicts for condition 2 an $f \sim 3.5$, and it is this lower value that will be assumed. P_T is the power loss due to the decay in the electron temperature, and reflects the observed decay in the pressure balance temperature. In equilibrium then one must have for the electrons,

$$-P_T = \frac{3}{2} Nk dT_e/dt$$

$$= P_{in} - P_r - (f - 2.5)NkT_{es}/\tau_N,$$

where T_{es} is the electron temperature of the FRC sheath region near the separatrix. From this equality it is found that $T_{es} = 113 \text{ eV}$ for condition 2. The T_e of 265 eV listed in Table I was measured on a flux surface which extends to roughly 2 cm inside the plasma edge. Assuming a linear drop in temperature, a crude estimate of the elec-

tron thermal diffusivity χ_e is $4 \text{ m}^2 \text{ s}^{-1}$. This is only a few times the classical value for condition 2. This χ_e would represent more than an order of magnitude improvement in confinement than previously observed [13], and is comparable to that observed in smaller tokamak experiments.

For a rigid-rotor equilibrium, the poloidal flux decay time τ_ϕ can be related to a field null resistivity $\eta(R)$ as $\tau_\phi = 1.5 \times 10^{-7} R^2 / \eta(R)$. The experimental $\eta(R)$ was compared to the classical cross-field Spitzer value, $\eta_{cl} = 1.6 \times 10^{-3} / [T_e(\text{eV})]^{3/2}$ (where $Z_{\text{eff}} = 1.3$), with the ratio being the anomaly factor. Since T_e and T_i both scale with B_e and inversely with n , the largest T_e occurred at the lowest fill pressure and the smallest value of the parameter s . Since all measures of confinement show a positive s scaling, the resistive anomaly is about 8 times classical for condition 1, but is roughly 40 for condition 2. Since the flux loss is always anomalous, and it was not possible to vary T_e independently from s , it is not clear what meaning should be given to the increase in the anomaly factor at small s and high T_e . It is, however, significant that the anomaly factor decreases with increasing s , for this had not been observed in previous experiments at high s [7].

The sharp increase in flux anomaly observed previously was attributed to increasing, destructive MHD activity, as s increased beyond 2. This was not observed in the

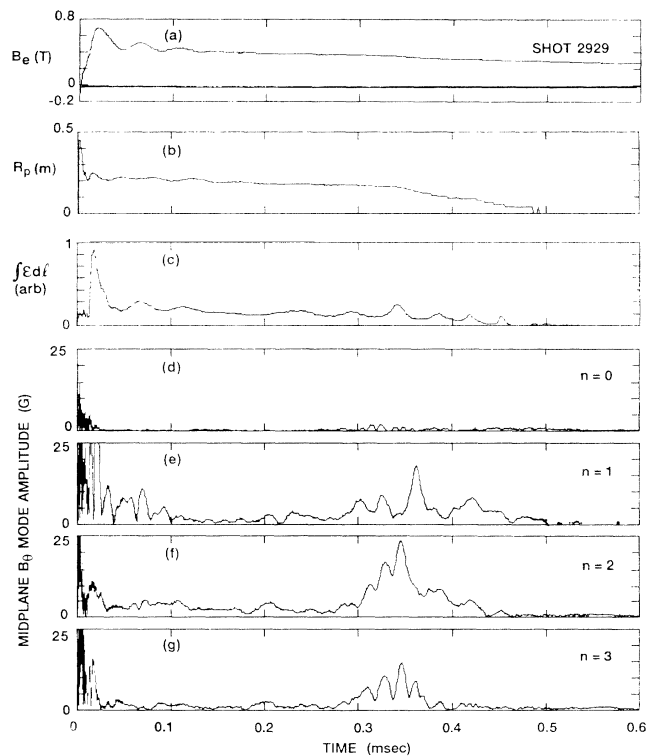


FIG. 3. Time history of (a) the external magnetic field; (b) the plasma radius; (c) integrated plasma emission ($\propto n_e^2$) along a central chord near the axial midplane; (d)-(g) the amplitudes of the $n=0, 1, 2$, and 3 Fourier components of FRC distortions.

LSX experiments when the proper formation sequence was followed. In light of the success at larger s in the LSX experiments, it is believed that the poor confinement observed in other experiments was due to the inability to form a stable equilibrium during formation at higher s . Although large B_θ signals could be observed during FRC formation, there was no correlation with confinement and the mode amplitudes observed.

This is illustrated in Fig. 3 which shows a time history for a discharge at high s . During the first 0.1 msec when there was significant B_θ signal, no degradation in confinement is observed ($\tau_N=0.71$ msec, $\tau_E=0.33$ msec). The average s and elongation E during this time were 4.4 and 5.3, respectively. The amplitudes plotted for the various azimuthal modes are for FRC separatrix movement having odd symmetry (as the $n=1$ tilt) about the axial midplane. In a previous experiment, poor confinement had correlated with the amplitude of the B_θ modes exceeding roughly 10 G for similar external fields, and was the basis for assuming that the tilt mode might be the underlying cause [7]. It would now appear that these signals merely reflected the more fluidlike nature of FRCs when $s > 2$. Only a small radial displacement (~ 1 cm) of the FRC separatrix would be required to generate a 10-G B_θ signal. Given the dynamic nature of the formation, one would expect to observe fluctuating B_θ signals as was observed in both experiments at higher s . From the random, oscillating nature of the observed B_θ signals though, a specific underlying instability does not appear to be the cause of the separatrix movement, nor does the appearance of these signals correlate with the quality of confinement in LSX.

In Fig. 3 the termination of the FRC was caused by the well documented $n=2$ rotational mode, which can be stabilized with external multipole fields. These fields were not employed during this discharge, so that the rotational mode was allowed to develop at about 0.3 msec, causing the termination of the FRC. The growing $n=2$ distortion can be observed as an oscillating signal by the side-viewing plasma emission detector [Fig. 3(c)], and is also clearly indicated by the growing $n=2$ mode amplitude derived from the B_θ array [Fig. 3(g)].

Stability to the ideal MHD tilt mode could be observed at s values as large as 8 with a marginal formation technique that generated a much more turbulent initial plasma. These high- s FRCs were obtained with fill pressures up to 20 mTorr, and the substantially greater initial energy required for ionization and heating resulted in equilibria that exhibited poorer confinement. Gross plasma distortions were observed end on during formation. These visible distortions as well as B_θ probe signals, however, were found to decrease during the equilibrium phase. The radial density profiles inferred from the emission data were much flatter for FRCs formed in this way, regardless of s value. The enhanced transport could be due to localized MHD activity, perhaps from higher-

order ballooning modes that are also predicted to be unstable for FRCs in the MHD limit [16].

Since it was possible to observe stability to gross MHD modes such as the tilt at any s value, the question must be asked then as to what may be the stabilizing mechanism at work in the FRC. Stability to the tilt in the MHD limit due to the Hall effect was found for $s < CE$, where for typical elongations observed on LSX ($4 < E < 6$) C is a constant, ≈ 0.23 [17]. The most recent work on MHD stability found a stabilizing influence from gyroviscous effects [18]. It was also found that a significant stabilizing effect came from the use of a much more realistic equilibrium in the analysis. For this equilibrium, the stability boundary was increased with $C \approx 0.5$. Many data points from LSX, however, still fall outside the region of stability. Recent work [19] using equilibria with a more hollow current profile, which appears to be more consistent with experimental data suggests an even greater MHD stability.

In summary, the new results from LSX indicate no stability limit due to any global MHD instability up to s values as large as 8. Continued strong confinement scaling is observed well into the MHD regime of $s \sim 5$. There is also strong evidence of considerably lower thermal transport inside the FRC separatrix for the larger plasmas formed in LSX.

-
- [1] M. Tuszewski, Nucl. Fusion **28**, 2033 (1988).
 - [2] D. J. Rej *et al.*, Phys. Fluids **29**, 852 (1986).
 - [3] H. L. Berk, H. Momota, and T. Tajima, Phys. Fluids **30**, 3548 (1987).
 - [4] M. N. Rosenbluth and M. N. Bussac, Nucl. Fusion **19**, 489 (1979); J. H. Hammer, Nucl. Fusion **21**, 488 (1981).
 - [5] J. T. Slough and A. L. Hoffman, Nucl. Fusion **28**, 1121 (1988).
 - [6] D. C. Barnes *et al.*, Phys. Fluids **29**, 2616 (1986).
 - [7] M. Tuszewski *et al.*, Phys. Fluids **B 3**, 2856 (1991).
 - [8] J. T. Slough and A. L. Hoffman, Phys. Fluids **B 2**, 797 (1990).
 - [9] K. F. McKenna *et al.*, Phys. Rev. Lett. **50**, 1787 (1983).
 - [10] S. Hamasaki and N. A. Krall, in *Conference Record of the IEEE International Conference on Plasma Science* (IEEE Publishing Service, Montreal, 1979), p. 143.
 - [11] A. L. Hoffman and J. T. Slough, Nucl. Fusion **26**, 1693 (1986).
 - [12] M. Tuszewski *et al.*, Phys. Rev. Lett. **66**, 711 (1991).
 - [13] D. J. Rej *et al.*, Nucl. Fusion **30**, 1087 (1990).
 - [14] D. J. Rej *et al.*, Phys. Fluids **27**, 1514 (1984).
 - [15] L. C. Steinhauer (to be published).
 - [16] J. M. Finn, Phys. Fluids **24**, 274 (1981).
 - [17] A. Ashida, H. Momota, and L. C. Steinhauer, Phys. Fluids **31**, 3024 (1988).
 - [18] L. C. Steinhauer and A. Ashida, Phys. Fluids **B 2**, 2422 (1990).
 - [19] L. C. Steinhauer (private communication).